Interhemispheric Coherence of Tropical Climate Variability: Effect of the Climatological ITCZ

Hideki OKAJIMA

Department of Meteorology, University of Hawaii, Hawaii, USA

Shang-Ping XIE

International Pacific Research Center and Department of Meteorology, University of Hawaii, Hawaii, USA

and

Atusi NUMAGUTI[1]

Graduate School of Environmental Earth Science, Hokkaido University, Sapporo, Japan

(Manuscript received 27 November 2002, in revised form 11 August 2003)

Abstract

The intertropical convergence zone (ITCZ) is the rising branch of the global Hadley circulation and often considered as the climatic axis of symmetry. A full-physics atmospheric general circulation model is coupled with an intermediate ocean model to investigate the effect of ITCZ's meridional configuration on the space-time structure of climate variability. In the control experiment where the model settles into a north-south symmetric climatology, strong interhemispheric interaction takes place and sea surface temperature (SST) anomalies are organized into an anti-symmetric dipole pattern with the equator as the nodal line. The trade winds intensify (weaken) over the anomalously cold (warm) side of the equator, indicative of a positive feedback between surface wind, evaporation and SST (WES). When the mean ITCZ is displaced into the Northern Hemisphere by perturbing the shape of continents, SST variability is significantly reduced at low-frequencies, especially with periods greater than 5 years, as a result of reduced interhemispheric interaction. The nodal line now coincides with the northward-displaced ITCZ, and the SST correlation across this nodal line is greatly reduced to a statistically insignificant level. Calculations with a simple baroclinic model of the atmosphere indicate that the departure of the climatic axis of symmetry from the geographic equator weakens the WES feedback and hence interhemispheric interaction.

Implications for tropical Atlantic variability are discussed. In particular, our result of ITCZ's modulation of interhemispheric interaction is consistent with the seasonality of cross-equatorial SST gradient variability: it peaks in boreal spring when the mean ITCZ is nearly symmetric about the equator and is significantly reduced in other seasons when the Atlantic ITCZ is displaced into the Northern Hemisphere.

1. Introduction

Ocean-atmospheric feedback is important for determining the spatial and temporal structure of climate variability. The El Niño and Southern Oscillation (ENSO) phenomenon is a good example. On the equator, where the Coriolis force vanishes and strong ocean upwelling exists, surface zonal winds, the thermocline depth and the sea surface temperature (SST) are closely coupled. Through this Bjerknes feed-

1 Deceased on 30 June 2001.

back, small perturbations amplify, resulting in coupled ocean-atmospheric variability that is confined to the equator. An equatorial maximum in interannual variance is found over both the Pacific and Atlantic, but the Atlantic maximum on the equator is highly seasonal and stands out only in boreal summer season of May, June, and July (Chiang et al. 2002).

In the tropical Atlantic, besides this equatorial mode of variability, off-equatorial SST anomalies play an important role in changing surface winds and the intertropical convergence zone (ITCZ). Many studies have shown that the Atlantic ITCZ is sensitive to cross-equatorial SST gradient in boreal spring season (Hastenrath 1991; Chang et al. 2001) and the anomalous shift of the ITCZ is a major cause of floods/droughts in Nordeste, Brazil (Nobre and Shukla 1996). Correlation analyses based on indices of cross-equatorial SST gradient usually result in a dipole pattern of SST anomalies with reversed signs across the climatological ITCZ (Servain 1991; Tanimoto and Xie 1999; Tanimoto and Xie 2002). Figure 1 shows an example of such correlation analysis. Noting that

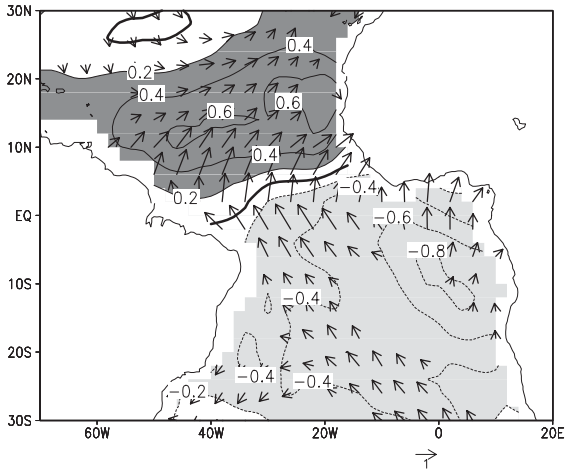

Fig. 1. Composite map for the cross-equatorial gradient mode based on NCEP Reanalysis for 1948–2001: sea surface temperature (contours; °C) and surface wind (vectors; m s^{-1}). Composite is taken as the difference between months when the zonal-mean (60°W–20°E) cross-equatorial wind velocity anomaly exceeds 0.2 m s^{-1} and falls below −0.2 m s^{-1}.

warm (cold) SST on either side of the equator is associated with the relaxed (intensified) trade winds, Chang et al. (1997) suggest that much of the dipole or cross-equatorial SST gradient variability is due to a positive feedback involving interaction of surface wind, evaporation and SST (WES), a mechanism that is originally proposed to explain the northward displacement of the climatological ITCZ of the Pacific (Xie and Philander 1994). The essence of this WES feedback is as follows. In response to an initial SST anomaly field of a dipole structure in the meridional direction, anomalous southerly winds are induced. The Coriolis force acts to turn the southerlies westward (eastward) in the Southern (Northern) Hemisphere, strengthening (weakening) the easterlies on the background and hence surface evaporation. The wind-induced changes in evaporative cooling would reinforce the initial SST anomalies.

The free coupled-mode arising from the WES feedback features an anti-symmetric dipole structure in the meridional direction (Chang et al. 1997; Xie 1999), implying a strong interhemispheric coherence in SST variability. Correlation of observed tropical Atlantic variability (TAV) between the north and south of the equator is negative, but is weak and statistically insignificant[1] (Houghton and Tourre 1992; Enfield and Mayer 1997; Mehta 1998), suggesting that the WES feedback is not the single dominant mechanism for TAV unlike the Bjerknes feedback that dominates the Pacific with the equatorially trapped ENSO (Neelin et al. 1998; Xie et al. 1999). An increasing number of studies suggest that the Atlantic cross-equatorial SST gradient (CESG) variability involves some air-sea interaction; in nearly all the atmospheric general circulation models (GCMs), the position of the Atlantic ITCZ is sensitive to CESG, although the meridional extent of WES-favorable wind response appears to vary from one model to another (Chang et al. 2000; Sutton et al. 2000; Okumura et al. 2001; Sutton et al. 2001). Okumura and Xie (2003)

1 There is evidence suggesting that significant negative coherence exists between the northern and southern tropics in the decadal band (Xie and Tanimoto 1998; Rajagopalan et al. 1998; Tanimoto and Xie 1999, 2002; Enfield et al. 1999), a notion supported by limited paleo-data analysis (Black et al. 1999).

suggest that this disagreement might arise from the difference in representation of the atmospheric boundary layer in models.

While a large body of literature exists on the Bjerknes mode and ENSO (Neelin et al. 1998; Wang et al. 1999; Fedorov and Philander 2000; Wang and An 2002), only a limited number of theoretical and modeling studies exist on CESG in general and WES in particular in the literature. Xie (1996) develops a simple theory for the WES mode and shows that it prefers westward phase propagation. While wind-induced evaporation provides positive feedback on SST, poleward advection by the mean Ekman flow in the ocean is a negative feedback (Xie 1999; Seager et al. 2000). Chang et al. (1997) suggest that the advection by the mean cross-equatorial ocean current provides the negative feedback switching the phase of CESG variability. Xie (1999) proposes the phase difference between wind speed and SST off the equator as an alternative mechanism for oscillation. Besides these mechanisms for free oscillation, external forcing such as ENSO and North Atlantic Oscillation (NAO) is probably important as well. Xie and Tanimoto (1998) and Chang et al. (2001) show that via the WES feedback, subtropical forcing like NAO can cause significant variability in CESG and, hence, the Atlantic ITCZ.

The WES feedback plays a key role in keeping the ITCZ to north of the equator over the Pacific and Atlantic (Xie and Philander 1994; Ma et al. 1996; Kimoto and Shen 1997; Xie and Saito 2001). Does this departure of climatic axis of symmetry from the equator have an effect on climate variability in the tropics? Observations hint at such a possibility; the nodal line of the observed gradient mode in the Atlantic is not on the equator but roughly coincides with the climatological ITCZ (Fig. 1; Servain 1991). The Atlantic ITCZ experiences large meridional excursion in an annual cycle; it is close or on the equator during the boreal spring and moves to as far as 10°N in boreal summer. This northward-displaced ITCZ is responsible for the boreal-summer peak of equatorial SST variance by enhancing the cross-equatorial southerlies and lifting the thermocline in the east. It remains to be investigated whether this seasonal march of the ITCZ has any effect on the CESG variability.

This paper reveals research on the effect of the climatological ITCZ on the space and time structure of climate variability. We use a hybrid coupled atmospheric GCM (HaGCM) developed by Xie and Saito (2001) under idealized conditions that are designed to isolate the WES feedback. Such a HaGCM has benefits in the ease in which results can be interpreted in relation to existing theories on one hand and with those from more sophisticated coupled GCMs on the other. As such, our emphasis is not on the realistic simulation of observed climate but rather on understanding a small number of processes and mechanisms under investigation. Such a simplified hybrid coupled modeling approach has proven fruitful in studying ENSO dynamics (Neelin et al. 1998). A main finding from this study is that the northward departure of the mean ITCZ from the equator substantially reduces the interhemispheric coherence in SST and wind variability, a result with a number of important implications for TAV research.

The rest of the paper is organized as follows. Section 2 describes the model and experimental designs. Sections 3 and 4 describe the climatology and temporal variability in the HaGCM, respectively. Section 5 is a summary and discusses the implications.

2. Model description

We use the HaGCM of Xie and Saito (2001), which consists of a full-physics, global atmospheric GCM and an intermediate ocean model. A brief description of the model follows; Please refer to Xie and Saito (2001) for details.

2.1 Atmospheric model

The atmosphere GCM was developed jointly at University of Tokyo's Center for Climate System Research (CCSR) and the National Institute for Environmental Studies (NIES) of Japan. The model solves primitive equations of motion in the spherical coordinates by the spectral method, and incorporates physical parameterizations for dry and moist convection, clouds, radiation, turbulence and ground hydrology. It is used widely in Japan as a community model under both realistic and idealized conditions (e.g., Inatsu et al. 2002). See Numaguti et al. (1995) and Numaguti (1999) for details and its performance. Here we use a

version with the triangular truncation at zonal wavenumber 21 (T21) in the horizontal and 20 sigma levels (L20) in the vertical. The choice of this horizontal resolution is a compromise between the need for long integrations [$o(100)$ years] and available computing resources. Okumura et al. (2001) show that this T21L20 version can reproduce reasonably well the atmospheric response to Atlantic SST anomalies in comparison to observations. More recently, Okumura and Xie (2003) repeat the same response experiments with a higher-resolution version (T42L23) and report very similar results to those with the T21L20 version.

2.2 Ocean model

HaGCM's oceanic component is an intermediate model based on Zebiak and Cane (1987). In particular, SST is determined by the horizontal advection, upwelling, surface heat flux, and horizontal diffusion,

$$\frac{\partial T}{\partial t} = -\mathbf{u}\cdot\nabla T - w\frac{T-T_e}{2H}\mathrm{P}(w) - \frac{Q}{\rho c_p H} - \kappa\nabla^2 T. \quad (1)$$

Here $\mathbf{u}$ is the horizontal velocity, w is the vertical velocity at the depth of the Ekman/mixed layer H with $\mathrm{P}(w)$ the Heaviside function, Q is the surface heat flux into the ocean with ρ and c_p being the density and specific heat at constant pressure of sea water, respectively, and κ is the diffusivity. The subsurface temperature to be entrained into the mixed layer, T_e, is determined by a hyperbolic function of thermocline depth (Dijkstra and Neelin 1995). Following Xie and Saito (2001), we simplify the ocean model by specifying a time-invariant thermocline depth field, $h(x, y)$. This removes the thermocline depth feedback and stabilizes the coupled ENSO mode that would otherwise give rise to large interannual variability—undesirable noise for our purpose of studying the meridional interaction. The thermocline depth field prescribed in this study is the steady-state solution to a linear reduced-gravity model forced with spatially uniform easterly wind stress of -0.03 N m^{-2}, a value representative of the equatorial zonal average in the Pacific and Atlantic. The thermocline tilts along the equator, being shallow in the east and along the eastern boundary. To be consistent with the fixed thermocline depth, only the surface Ekman flow is used to advect SST and to compute upwelling velocity. Mechanisms for developing CESG, including surface heat flux adjustment (Xie and Philander 1994; Chang et al. 1997) and Ekman upwelling (Chang and Philander 1994), are thus retained in this simplified ocean model.

2.3 Coupling

The ocean and atmosphere models exchange information once a day. Each day, the atmospheric GCM updates its SST boundary condition from the ocean model output and meanwhile passes daily-average fields of surface wind stress and heat flux to the ocean. The atmospheric wind stress drives ocean Ekman flow and upwelling while surface heat flux directly forces SST. The heat flux at the ocean surface is decomposed into four components:

$$Q = Q_S - Q_L - Q_H - Q_E. \quad (2)$$

Here the absorbed solar (Q_S) and net upward long-wave (Q_L) radiation is computed with the AGCM's radiation code and varies interactively with water vapor and cloud fields. The sensible (Q_H) and latent (Q_E) heat fluxes are computed using the atmospheric GCM's aerodynamic bulk formulas (Miller et al. 1992). As an important deviation from the original Zebiak-Cane model that treats surface heat flux as a Newtonian damping, equation (1) incorporates both the WES and cloud-SST feedbacks.

2.4 Boundary conditions

The atmospheric model is global. In the control run, two continents that are 40° wide and 140° apart in longitude are placed in the model, with their coasts running along meridians (hereafter *Sym-run*). In one of the ocean basins enclosed by these continents (135°E–85°W), SST evolves interactively with the atmospheric GCM between 30°S and 30°N. Poleward of 30° and in the other ocean basin, SST is prescribed with a zonally uniform, equatorial symmetric distribution (upper panel of Fig. 2). The ocean model in the active basin is solved by time stepping at a 3° longitude and 1° latitude resolution. Over the continents, surface temperature and soil moisture are computed interactively according a bucket model of land hydrology with a constant surface albedo of

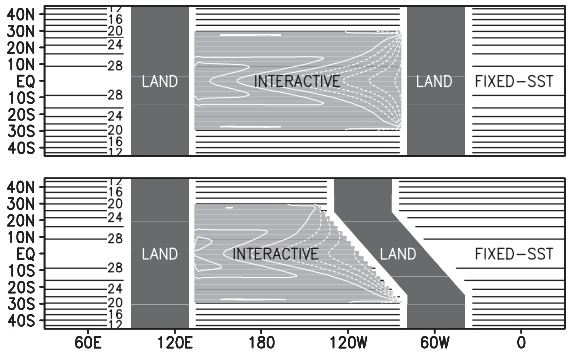

Fig. 2. Land-sea distributions in the HaGCM for the symmetric (upper) and asymmetric (lower) runs, with dark shade denoting the continents. SSTs are prescribed (contours; °C) in a distribution symmetric about the equator in one basin and evolve interactively in another (light shade). White contours in the active ocean basin are for the prescribed thermocline depth (deviation from zero with intervals of 15 m).

0.25 that is typical of grass land. In the second experiment, we perturb the climate away from the equatorial symmetry by tilting the eastern continent of the active ocean northwestward at a 45° angle (*Asym-run*: lower panel of Fig. 2).

For simplicity, the solar insolation is set to its equinox distribution, which is perfectly symmetric about the equator. Both runs are integrated for 72 years. The averages for the last 70 years are taken as climatology and deviations from it are called anomalies.

The above HaGCM was originally set up to study how continental asymmetry triggers the northward displacement of the Pacific ITCZ, but the subsequent analysis led to a new focus, namely interhemispheric coherence of temporal variability. The model also was run for a short period of time in a narrower Atlantic-like basin but turned out to produce too weak an equatorial tongue, a problem common to many coupled GCMs (P. Chang 2002, personal communication). Here, only results from the runs with a Pacific-size active ocean domain will be presented. A recent observational study suggests that a meridional gradient mode exists in the tropical Pacific, much like the more familiar one in the Atlantic (J.C.H. Chiang and D.J. Vimont, 2003: Analogous Pacific and Atlantic meridional modes of tropical atmosphere-ocean variability, unpublished manuscript). We will discuss our model results in relation to TAV since it is better studied and documented than the Pacific meridional gradient mode.

3. Climatology

An equatorially symmetric climate forms in the Sym-run (Fig. 3). There is a major warm pool that occupies the western half of the equatorial basin with SST greater than 28°C. The easterly trade winds prevail over most of the basin. Along the equator, wind-induced upwelling maintains a cold tongue in the eastern half of the basin except near the eastern boundary, where the winds are westerly on the equator and converge onto the warmer continent. In the meridional direction, the cold tongue divides two local SST maxima, one on each side of the equator.

With a northwestward tilted eastern continent, the climate over the active ocean shifts into an asymmetric state, with warm water (>28°C) and the ITCZ confined to the Northern Hemisphere. As discussed in Philander et al. (1996) and Li (1997), the tilted coastline favors the Southern Hemisphere for upwelling; the coastal winds blow alongshore (offshore) south (north) of the equator. This asymmetry in coastal upwelling triggers a coupled WES wave front that propagates westward and establishes climatic asymmetry on the way (Xie 1996; Xie and Saito 2001). The winds are weak along the warm band north of the equator that supports the ITCZ there, forming the doldrums, while high winds are found over the colder water on the other side of the equator. This asymmetry in wind speed is indicative of the symmetry-breaking effect of the WES feedback.

The climatology in the Asym-run resembles that observed over the Pacific, a result partly due to our imposing a coastline tilt greater than the west coast of real South America. The improved realism over the Sym-run is not limited to the permanent displacement of the ITCZ into the Northern Hemisphere but also includes the removal of unrealistic warm water in the far east of the equatorial basin. This warm bias in the eastern equatorial Pacific is a common problem in most of coupled GCMs (Mechoso et al. 1995) and may be related to the failure of these models to keep their ITCZ north of

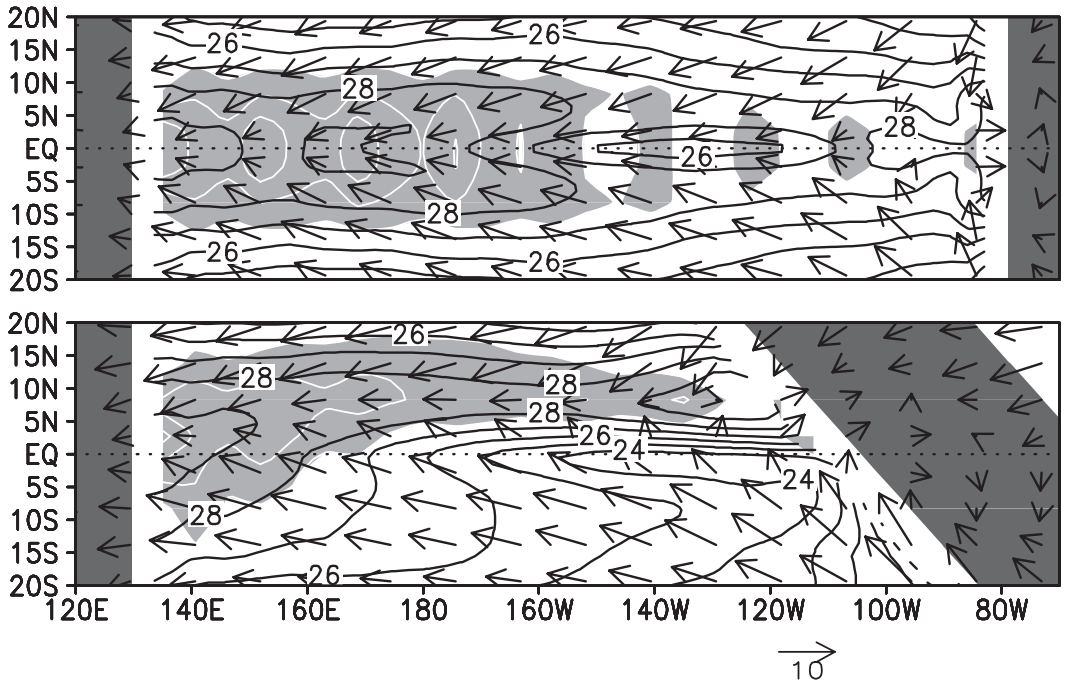

Fig. 3. Climatologies of SST (contour interval 1°C), surface wind (vectors; scaled to 10 m s^{-1}), and precipitation (shade > 4 mm day^{-1} with white contours at intervals of 4 mm day^{-1}) for the Sym-run (upper) and Asym-run (lower).

the equator. In our HaGCM, the strong southerly winds that converge onto the northerly ITCZ induce upwelling south of the equator (Chang and Philander 1994) and strengthen the equatorial cold tongue on the basin scale. Xie (1998) discusses how the onset of local cross-equatorial winds in the east can cause a basin-wide adjustment in the equatorial cold tongue.

4. Temporal variability

Despite a constant insolation in time, significant temporal variability is found in both runs of the HaGCM, with well-organized spatial structures. This section investigates the mechanisms for such temporal variability and how the differences in climatology affect its time-space structure. We start with the simpler Sym-run and then move onto the Asym-run.

4.1 Symmetric run

Pronounced SST variability develops in the Sym-run (Fig. 4) and at any given time, the model climate is rarely, if ever, in an equatorial symmetric state (with anomalies vanishing in both hemisphere). As noted by Xie and Saito (2001) in a much shorter (9 years) integration, the SST anomalies are roughly anti-symmetric about the equator. This dominance of meridional dipole mode is a result of holding the thermocline depth time-invariant and suppressing the Bjerknes ENSO mode, allowing us to focus on the ocean-atmosphere interactions through surface processes (heat flux and Ekman dynamics).

In the first 20 years of the integration, the SST dipole seems to display a preferred decadal timescale, but the spectral analysis of cross-equatorial wind velocity (V_{eq})—a simple measure of the equatorial asymmetry—does not produce such a decadal peak (solid line in Fig. 5). The spectrum is white at high frequencies and begins to show a reddening tendency for periods greater than 0.5 year. There is a broad spectral peak around periods of 2–3 years, which seems to stand out of background red spectra. This causes an abrupt increase of power around the 2-year period. The spectral power at periods of a few years and longer is 100 times greater than that at the high-

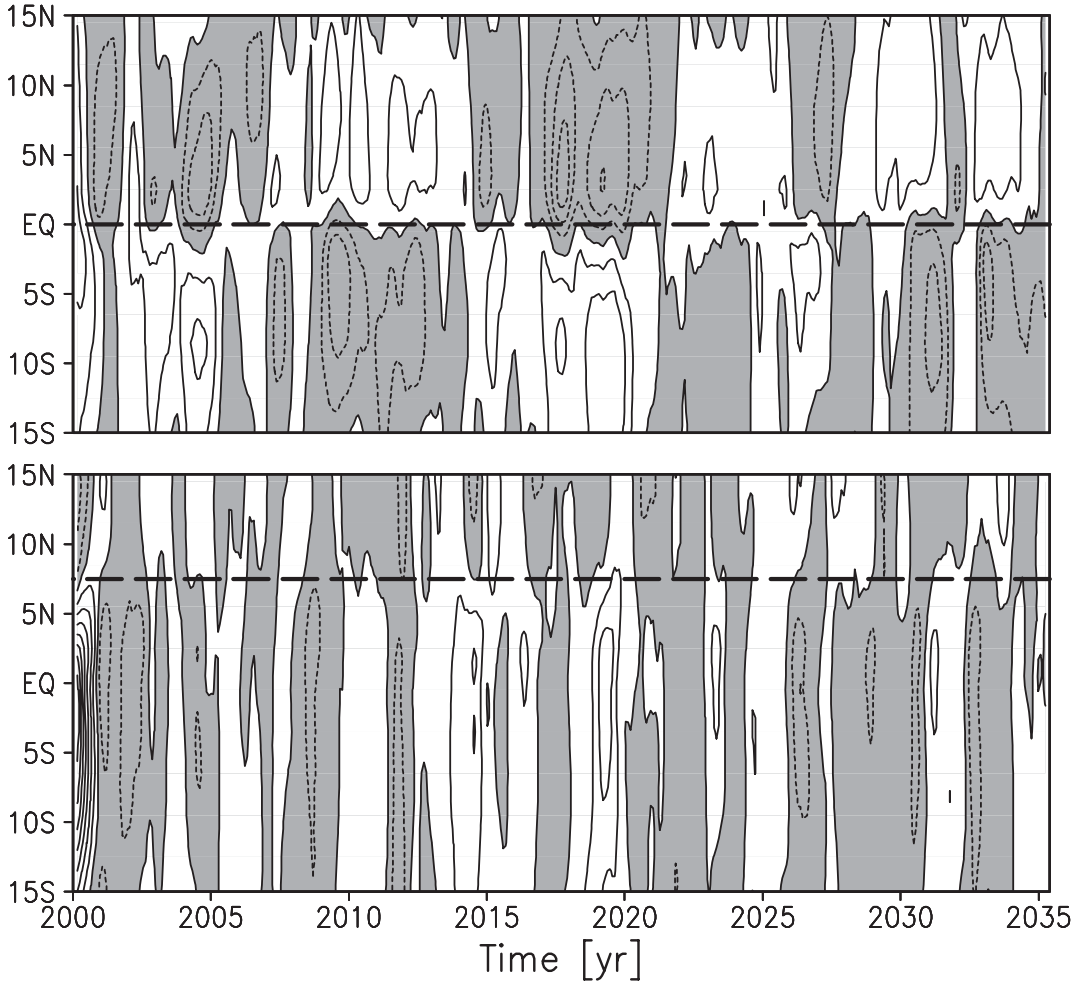

Fig. 4. Latitude-time diagrams of zonal-mean (135°E–85°W) SST anomaly (contour interval 0.3°C, negative values are shaded) for the Sym-run (upper) and Asym-run (lower). Thick dashed line indicates the latitude of the climatological ITCZ ($\bar{v} = 0$). A 7-month running mean is applied for clarity.

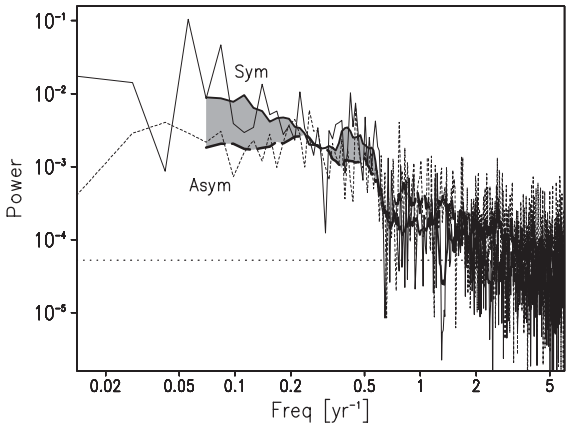

Fig. 5. Power spectrum density of cross-equatorial meridional wind velocity averaged in 135°E–85°W and 3°S–3°N for the Sym-run (solid line), and 135°E–120°W and 5°N–10°N for the Asym-run (dashed), as a function of frequency (year^{-1}). Thick lines are the 9-point running mean. Positive differences in power, Sym-run minus Asym-run, are shaded. The dotted line indicates the "white noise" level, estimated from the uncoupled AGCM run.

frequency end. In the inactive ocean basin, the same V_{eq} spectrum is virtually white at all frequencies (not shown). The enhanced power of the atmospheric spectrum at interannual timescales in the active ocean basin is indicative of the positive feedback, in contrast to stochastic models for the mid-latitude ocean that redden the ocean spectra but assume a white-noise atmosphere with little feedback from the ocean. Chang et al. (1997) and Xie and Tanimoto (1998) show that the WES feedback gives rise to coupled variability of lower frequencies than the ocean thermal damping scale (<1 year).

The strong interhemispheric coherence is further illustrated by correlations of SST and surface wind velocity with zonal-mean SST in the 0–15°S latitudinal band. Strong SST correlation of the opposite sign is found in the Northern Hemisphere (Fig. 6). Anomalous southerlies blow from the colder to the warmer hemisphere, which under the Coriolis force, are responsible for the enhanced southeasterly trades south of the equator and reduced northeasterly trades to the north. Such a pattern with the strengthened (relaxed) trade winds over the negative (positive) SST anomalies is characteristic of the WES feedback that is responsible for strong low-frequency variability in the model. In addition to the wind-induced evaporation changes, open-ocean upwelling with opposite signs across the equator that is induced by cross-equatorial wind changes also contributes to the SST dipole. In the meridional direction, the SST extrema are displaced poleward of the wind speed ones, indicative of advection by the poleward mean Ekman flow. See Xie and Saito (2001) for a more detailed discussion of ocean heat budget in a similar model (their Fig. 8).

In the zonal direction, the correlation fields maintain the same signs, in support of the result of a linear theory that the WES instability peaks at zonal wavenumber zero (Xie et al. 1999). Wind anomalies are weak on the eastern edge but extend far west of the western edge of the SST anomalies, a zonal asymmetry due to the westward propagation of long atmospheric Rossby waves. This westward shift of anoma-

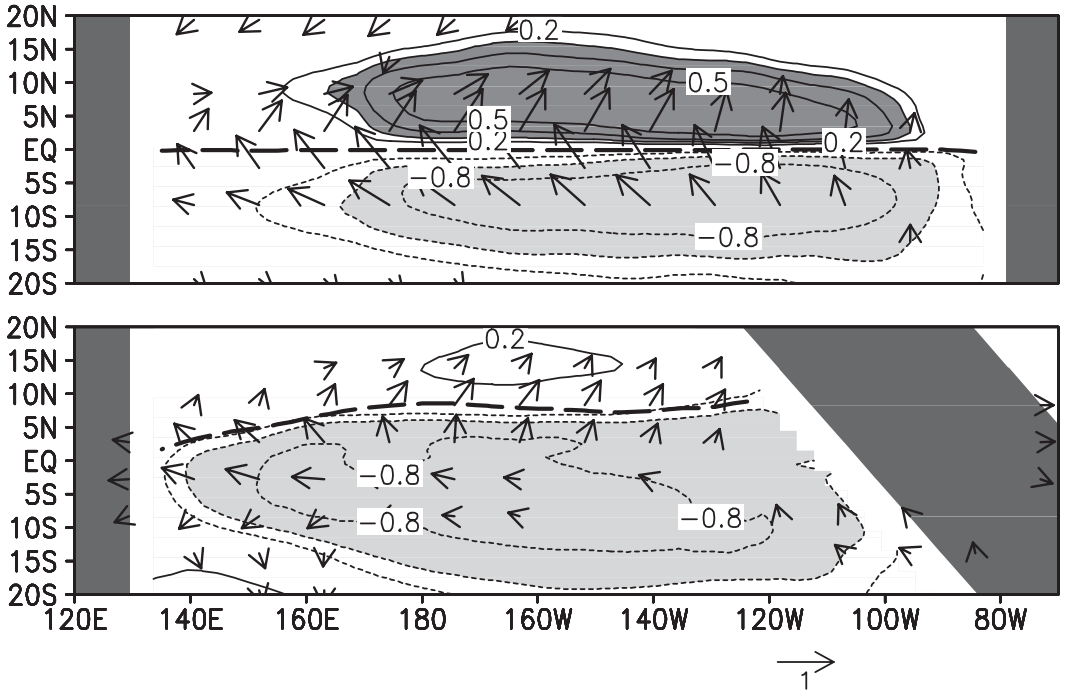

Fig. 6. Correlations with SST averaged zonally across the basin and in 0–15°S: SST (dark shade > 0.3, light shade < −0.6; contours are −0.8, −0.6, −0.4, 0.2, 0.3, 0.4, 0.5), and surface wind velocity (vectors, scaled by 1). The thick dashed line indicates the climatological ITCZ ($\bar{v} = 0$). The signs of correlations are reversed.

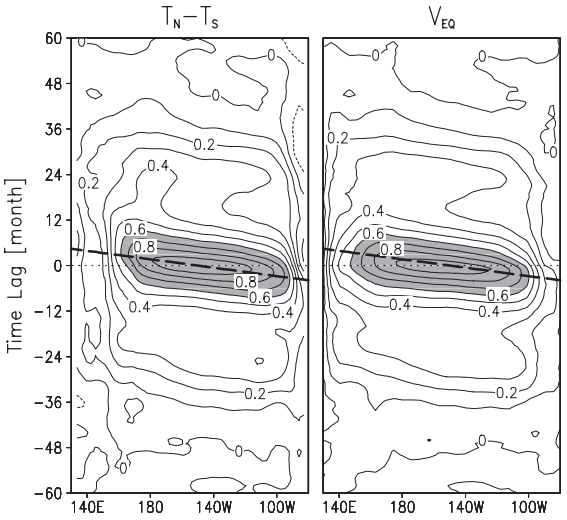

Fig. 7. Time-lagged correlations as a function of longitude and lag with SST difference between 0–10°N and 0–10°S averaged in 160°W–140°W: cross-equatorial SST gradient (left panel) and meridional wind at the equator (right). Correlation coefficient greater than 0.6 is shaded. The thick dashed line indicates the best-fit westward phase propagation.

lous wind causes a slow westward propagation of the coupled variability (Fig. 7), as described by a linear theory (Xie 1996). The cross-basin time for the westward propagation is about 1 year, comparable to the time scale of the rapid decay of correlations near lag zero. The zero-crossing of correlations occurs at a much larger lag of 4 years.

The dominance of the dipole mode in this HaGCM is reaffirmed in the SST root-mean-squared (rms) variance field (Fig. 8). Much consistent with the correlation map, a variance maximum is located on each side of the equator while a distinct minimum forms along the equator. The variance decreases rapidly west of 180° because of the reduction in the mean easterly wind velocity, a necessary condition for the WES feedback (Xie and Philander 1994), and possibly because of the negative feedback between SST and deep convective clouds over the warm pool.

4.2 Asymmetric run

The northward displacement of the climatological ITCZ in the Asym-run causes marked changes in the time-space structure of low-

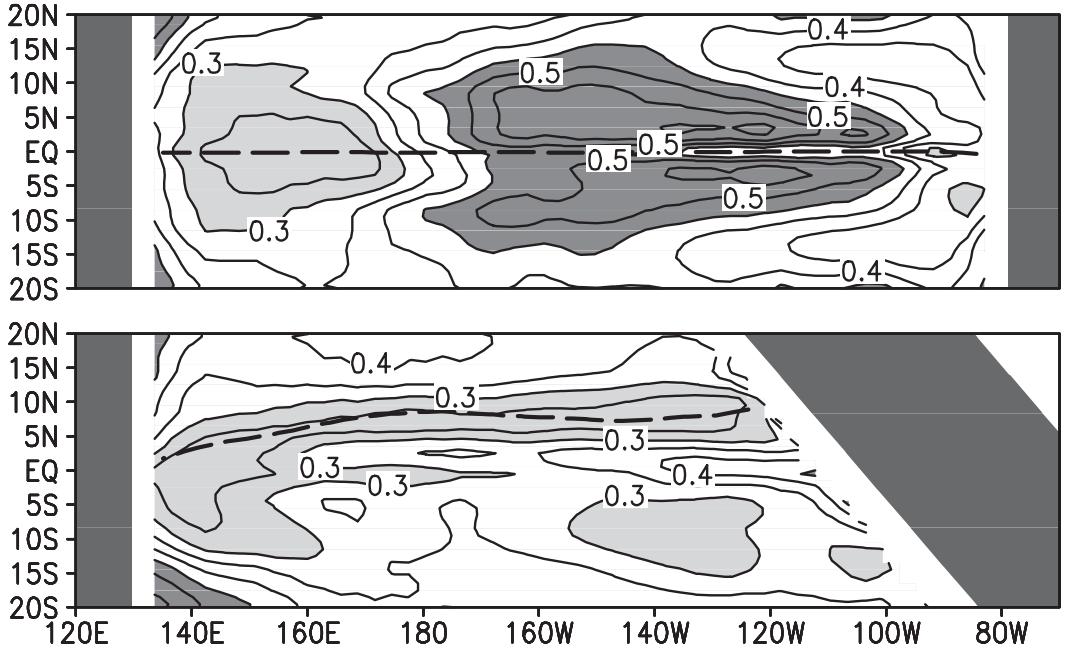

Fig. 8. Root-mean-square variance of SST (dark shade > 0.45, light shade < 0.3°C). The thick dashed line indicates the climatological ITCZ ($\bar{v} = 0$).

frequency variability. In the time-latitude section of SST anomalies (Fig. 4, lower), the latitude of minimum SST variability apparently shifts and is now located at the climatological ITCZ. This collocation of the low variability zone with the ITCZ is confirmed in Fig. 8. The mean ITCZ is selected as the nodal line for SST variability partly because of the weak climatological winds in the ITCZ that reduce the effect of wind fluctuations on SST through evaporation. The negative feedback between the radiative effect of ITCZ clouds and underlying SST also acts to stabilize SST there. Tanimoto and Xie (2002) report such a negative cloud-SST feedback near the Atlantic ITCZ based on historical ship observations.

Besides this northward shift of the nodal line, the rms SST variance decreases significantly within 15°S–15°N. Near the centers of action for the meridional dipole in the Sym-run, the reduction in rms variance is particularly pronounced, suggesting a weakening of the WES feedback that give rise to the strong interhemispheric interaction in the Sym-run in the first place. The northward-displaced ITCZ is an apparent axis of symmetry for model climate variability; we choose the meridional wind velocity here at 8°N, V_{ITCZ}, as a measure of cross-ITCZ interaction. Its spectrum (dashed line in Fig. 5) shows that this cross-ITCZ interaction is significantly reduced in the lower-frequency band with periods greater than 5 year. At the 10-year period, the power (smoothed curve) for cross-equatorial wind in the Sym-run is five times greater than that for cross-ITCZ wind in the Asym-run while at the high-frequency end (period shorter than 1 year) the opposite is true—the power is consistently greater in the Asym-run. It is unclear at this time why the Asym-run has higher variability across the axis of symmetry, but the high convective activity in the ITCZ may be a reason. In the Sym-run, convection is rather suppressed along the equator (the climatic axis of symmetry).

Interhemispheric coherence is visibly reduced in Fig. 4. Cold events south of the mean ITCZ are not always associated with warm events to the north and vice versa as they are in the Sym-run. The correlation analysis based on the same area-average SST index as in our Sym-run analysis confirms this reduction in the interhemispheric interaction. The correlation coefficients north of the ITCZ drop to only about 0.2 (Fig. 6), a value similar to the interhemispheric SST correlation reported by Houghton and Tourre (1992). Interestingly, however, the SST anomalies are still organized into the basin scale in the zonal direction and the half-tropical scale in the meridional, a pattern similar to observed TAV.

The attendant wind anomalies help maintain the SST correlation pattern in Fig. 6. For example, the weakened northeasterly trades north of the ITCZ reduce the evaporative cooling and thereby warm SST there. South of the equator, the southeasterlies are generally increased, helping cool SST there. As a major difference from the Sym-run, the anomalous cross-equatorial southerlies now cool the water between the ITCZ and equator by strengthening the mean southerlies and increasing surface evaporation there. These cross-equatorial winds force surface water to flow northward and, thereby, intensify the open-ocean upwelling south of the equator and the associated cooling, resulting in the SST variance maximum in the eastern equatorial basin in Fig. 8.

4.3 Simple model analysis

To illustrate how ITCZ's departure from the equator affects interhemispheric interaction, we consider the wind-induced evaporation feedback on SST as suggested by the correlation map in Fig. 6. Here we are aiming at a qualitative understanding and use a simple SST equation of Xie (1997)

$$\frac{\partial T'}{\partial t} = aU' - bT', \tag{3}$$

where U' is the perturbation zonal wind velocity, a and b are both positive quantities obtained by linearizing the latent heat flux term under the mean easterly wind condition. A positive wind anomaly would reduce the mean easterly wind speed and hence increase SST. Thus, aU' represents the wind-induced evaporation feedback and $-bT'$ is the Newtonian cooling resulting from the SST dependence of surface evaporation. Multiplying both sides with T' and integrating over the whole domain results in the following "energy" equation

$$\frac{1}{2}\frac{\partial}{\partial t}\overline{T'^2} = a\overline{U'T'} - b\overline{T'^2}, \tag{4}$$

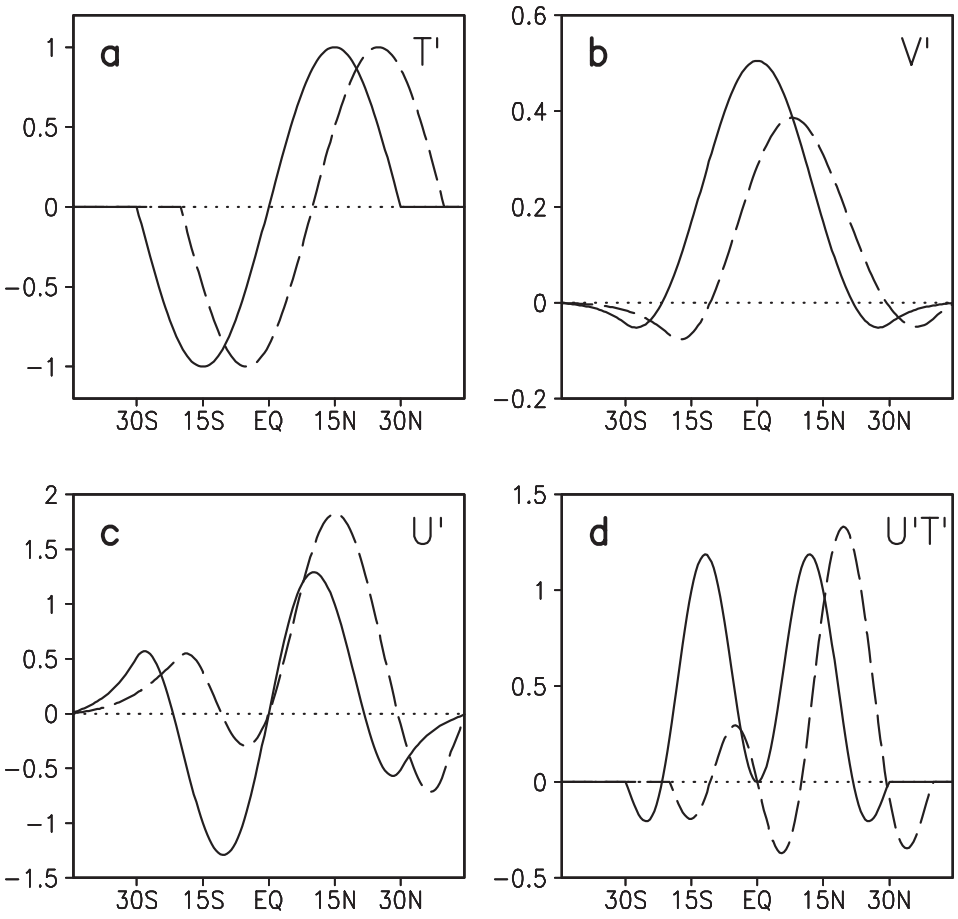

Fig. 9. Linear response to (a) anti-symmetric SST anomaly (°C): (b) meridional and (c) zonal wind velocity (m s^{-1}), and (d) destabilizing factor. Axises of the anti-symmetric SST anomaly are on the equator (solid) and at 10°N (long dashed).

where the overbar denotes the meridional average. It follows that the term $U'T'$ is a measure of the WES feedback and controls the growth of the positive quantity T'^2.

In the following we estimate this atmospheric feedback term onto a SST distribution shown in Fig. 9:

$$T' = T_0 \sin \pi\left(\frac{y - y_0}{Y}\right) \quad \text{for } (-Y < y - y_0 < Y);$$

otherwise $T' = 0$.

Here y_0 is the nodal point or axis of symmetry of this SST dipole, which our HaGCM experiments show is the latitude of the mean ITCZ. We use the linear, axis-symmetric model of Mastuno (1966) and Gill (1980):

$$\varepsilon U' - \beta y V' = 0,$$

$$\varepsilon V' + \beta y U' = -\frac{\partial \Phi'}{\partial y},$$

$$\varepsilon \Phi' + C_A^2 \frac{\partial V'}{\partial y} = -Q',$$

where ε is the atmospheric damping rate, β is the latitudinal gradient of the Coriolis parameter, Φ is the geopotential, and C_A is the atmospheric long gravity wave speed. For simplicity, zonal symmetry is assumed. The surface wind response is computed by letting the diabatic heating to the atmosphere Q' be proportional to SST anomalies:

$$Q' = K_Q T',$$

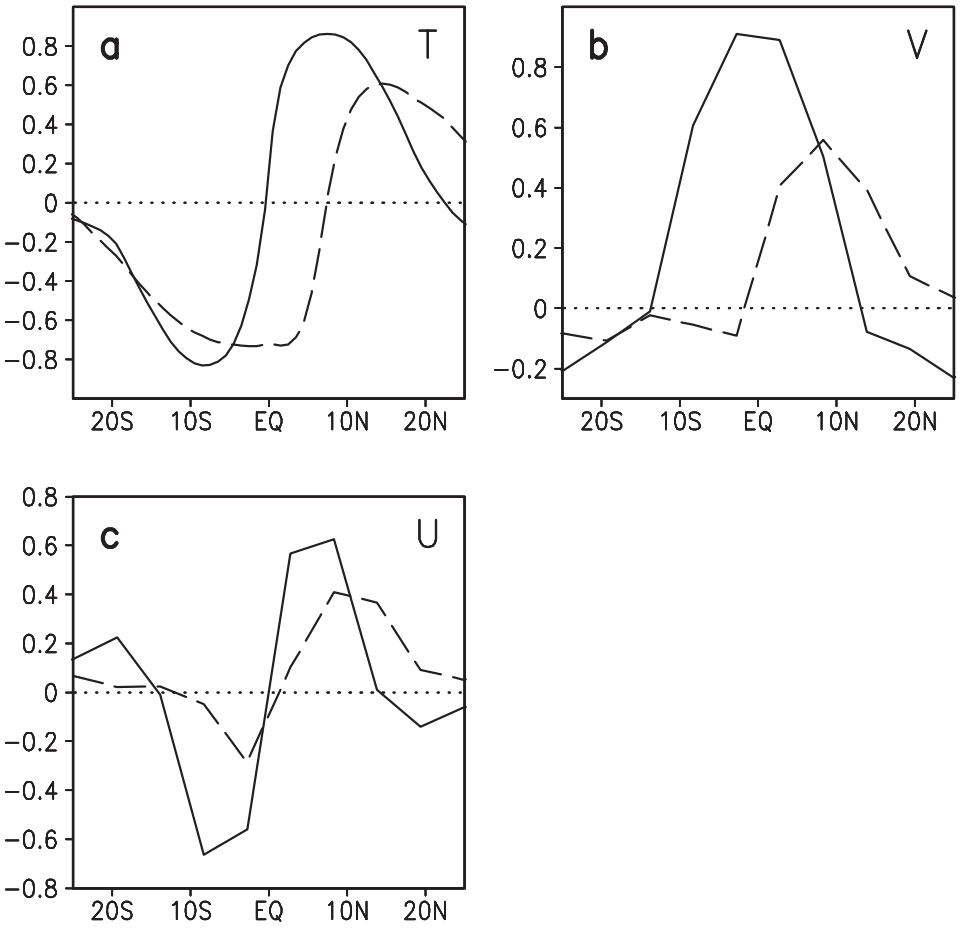

Fig. 10. Same as Fig. 9 but for the result of HaGCM experiments: Sym-run (solid) and Asym-run (long dashed). Correlation coefficients of: (a) SST, (b) meridional and (c) zonal wind velocities, with the SST difference between 0–15°N and 0–15°S for the Sym-run, and 10–25°N and 10°S–5°N for the Asym-run, averaged zonally in 170°E–130°W.

where K_Q is the coupling coefficient. We use $T_0 = 1°\mathrm{C}$, $Y = 30°$, $\varepsilon = 2$ day^{-1}, $\beta = 2.28 \times 10^{-11}$ m^{-1} s^{-1}, $C_A = 45$ m s^{-1}, and $K_Q = 6 \times 10^{-6}$ W K^{-1}.

In the equatorial region, anomalous cross-equatorial flow can be considered as the direct response of the atmosphere to the SST gradient of the imposed dipole, taking a bell-shaped curve centered at $y = y_0$ (Fig. 9b). Under the symmetric ITCZ ($y_0 = 0$; solid lines in Fig. 9), the zonal wind anomaly induced by the Coriolis force is also a dipole roughly collocated with the SST dipole, resulting in large SST-wind co-variance on both sides of the equator that would act to amplify the SST dipole if SST were allowed to vary.

With the mean ITCZ displaced northward ($y_0 = 10°$N; dashed lines in Fig. 9), in addition to a northward translation, the peak of the bell curve for V' decreases because of the resistance by stronger earth rotation against ageostrophic flow. Associated with the reduction in V' near the equator, the induced easterly wind anomaly shows a much weaker peak to the south, and so does the SST-wind co-variance there. This weakened co-variance peak is further offset by negative co-variance between the equator and ITCZ, where U' remains positive but T' is now negative. As a result, the meridional-mean co-variance is significantly reduced compared to the case with the SST dipole centered on the equator.

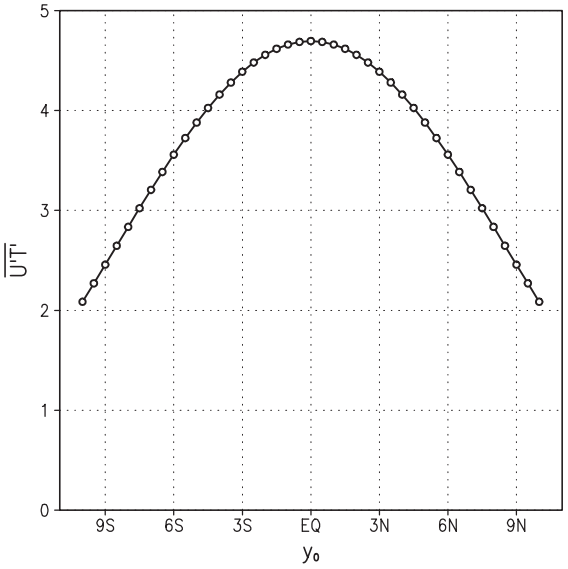

Fig. 11. Area integral of $U'T'$ as a function of y_0.

Figure 10 shows SST and wind regressions upon a CESG index in the Sym-run and Asym-run. The overall wind structures are similar to those in the Matsuno-Gill model, including the reduced cross-equatorial wind anomalies in the Asym-run. South of the equator, zonal wind anomalies are weaker in the Asym-run than the Sym-run, reducing the SST-wind covariance. The cross-ITCZ asymmetry in the U'-T' covariance—high to the north and low to the south (Figs. 9 and 10)—seems consistent with larger SST variance in 15–20°N than in 15–20°S (Fig. 8).

Figure 11 shows the meridional-mean SST-wind co-variance as a function of y_0. The wind feedback onto the SST as measured by this covariance peaks with the symmetric ITCZ and decreases monotonically with the ITCZ moving away from the equatorial symmetry. With the ITCZ at 10°N, the wind feedback is only 44% of that with a symmetric climatology. This rapid reduction in feedback with y_0 seems to offer a qualitative explanation of reduced interhemispheric interaction in the Asym-run of our HaGCM.

5. Discussion

The ITCZ is often viewed as the climatic axis of symmetry since it controls the rising branch of the interhemispheric Hadley circulation. The results of this study cast another role for the ITCZ, as the axis of symmetry for climate variability involving ocean surface processes (such as heat flux and Ekman dynamics). In a symmetric climate, the geographic equator coincides with the climatic axis of symmetry. Strong interhemispheric interaction takes place and pronounced dipole variability results in our HaGCM, with the equator as the nodal line. When the ITCZ is displaced north of the equator, by contrast, this departure of climatic axis of symmetry ($\bar{v} = 0$) from the geographic one ($f = 0$) weakens interhemispheric coherence of interannual variability in the model, with the ITCZ as the nodal line instead. The reduced SST variability at the ITCZ is a result of weak background wind—unfavorable for the WES feedback—and a negative cloud-SST feedback. Our simple model result shows that this displacement of the nodal line from the equator weakens the WES feedback south of the ITCZ and, hence, is unable to maintain the SST dipole centered at the ITCZ.

Throughout the year, SST variance generally reaches one minimum near the maximum climatological SST or ITCZ (Fig. 12), consistent with the Asym-run results. Our model results suggest that this climatic asymmetry is a reason why interhemispheric correlation is much weaker than predicted by previous theoretical studies of the WES mode, which all assume the equator as the climatic axis of symmetry. In the annual cycle, CESG variability is known to show strong seasonality, strong in boreal spring and weak in other seasons. This seasonality also seems consistent with our conclusion that the meridional configuration of the mean ITCZ dictates interhemispheric coherence. In boreal spring, the Atlantic climate is nearly symmetric about the equator and cross-equatorial interaction on interannual timescales—as measured by the variance of both CESG and cross-equatorial wind velocity—is strong (Fig. 12). In other seasons, the ITCZ is confined to the Northern Hemisphere and the cross-equatorial variability is low.

The tropical Atlantic is not a closed system but instead receives strong forcing from the outside. The NAO is the strongest in boreal winter and can affect TAV via its subtropical pole's modulation of the northeasterly trades

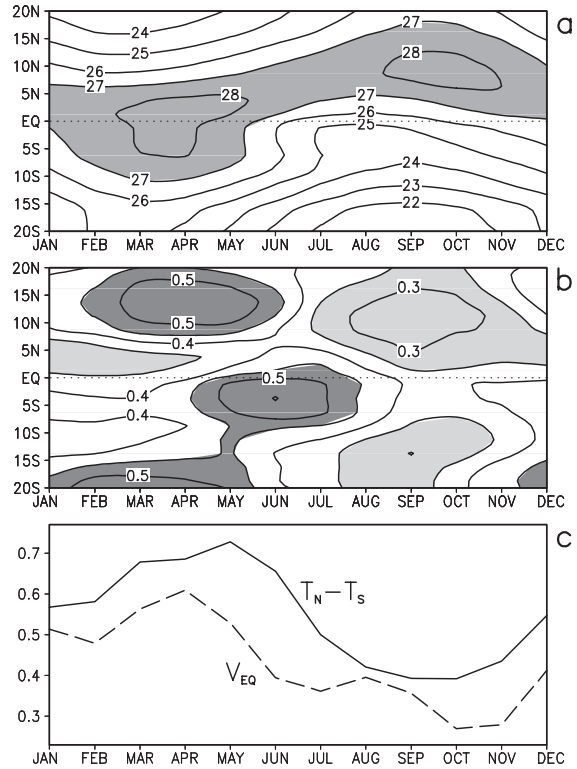

Fig. 12. Time-latitude sections of observed annual cycle of (a) SST (shade > 27°C), and (b) SST variance (dark shade > 0.45°C, light shade < 0.35°C). (c) Variances of meridional SST gradient (solid) and cross-equatorial wind (dashed). Zonal means in 60°W–20°E are used based on the NCEP Reanalysis for 1948–2001. SST gradient is calculated by taking difference between NH (10°N–20°N) and SH (15°S–5°S).

in the North Atlantic (Xie and Tanimoto 1998; Chang et al. 2001; Czaja et al. 2002). Both the ENSO and its teleconnection to North America and the North Atlantic are the strongest in the boreal winter as well (Enfield et al. 1999; Klein et al. 1999). The strong external forcing from these sources in boreal winter also seems to contribute partly to the boreal-spring peak of CESG variance (Chiang et al. 2002).

There are several caveats for direct application of our results to the real Atlantic. Most importantly, the subsurface ocean dynamics are removed in our HaGCM, which has allowed us to focus on surface feedbacks. With active ocean dynamics included, the Bjerknes feedback will enhance equatorial variability and interact/interfere with the WES mode discussed here. In fact, in the real Pacific that has a large zonal size, this equatorial Bjerknes mode overwhelms the WES variability. Our model results show that by removing the thermocline depth feedback and hence weakening the Bjerknes feedback, the WES feedback has a chance to manifest itself and becomes dominant even in a large ocean basin. While unique in the real climate system, the relative strength of the Bjerknes and WES feedbacks may vary from one coupled model to another. For example, a meridional dipole mode of coupled variability appears in the coupled GCM of Meteorological Research Institute of Japan, with anomalies of SST and surface wind in distributions consistent with the WES feedback (Yukimoto et al. 2000). A recent observational study suggests that the tropical Pacific has a meridional gradient mode with a coupled SST-wind structure similar to its counterpart in the tropical Atlantic (J.C.H. Chiang and D.J. Vimont 2003, unpublished manuscript).

Acknowledgments

The first two authors dedicate this paper to Atusi Numaguti for spearheading the development of the CCSR/NIES AGCM version 5.4 and his generosity in opening his code to the Japanese university community. The authors would like to thank M. Watanabe for helpful discussion, K. Saito for technical assistance, and J.C.H. Chiang and anonymous reviewers for useful comments. GFD-DENNOU Library and GrADS were used for analysis and graphics. This work is supported by NOAA CLIVAR Program (NA17RJ1230), NSF (ATM01-04468), JSPS Grant-in-Aid for Scientific Research (12440123), CCSR of University of Tokyo, and Frontier Research System for Global Change. IPRC contribution #235 and SOEST contribution #6256.

References

Black, D.E., L.C. Peterson, J.T. Overpeck, A. Kaplan, M.N. Evans, and M. Kashgarian, 1999: Eight centuries of North Atlantic Ocean atmosphere variability. *Science*, **286**, 1709–1713.

Carton, J., X. Cao, B.S. Giese, and A.M. da Silva, 1996: Decadal and interannual SST variability

in the tropical Atlantic Ocean. *J. Phys. Oceanogr.*, **26**, 1165–1175.

Chang, P. and S.G.H. Philander, 1994: A coupled ocean-atmosphere instability of relevance to the seasonal cycle. *J. Atmos. Sci.*, **51**, 3627–3648.

———, L. Ji, and H. Li, 1997: A decadal climate variation in the tropical Atlantic ocean from thermodynamic air-sea interactions. *Nature*, **385**, 516–518.

———, ———, and R. Saravanan, 2001: A hybrid coupled model study of tropical Atlantic variability. *J. Climate*, **14**, 361–390.

Chiang, J.C.H., Y. Kushnir, and A. Giannini, 2002: Deconstructing Atlantic ITCZ variability: influence of the local cross-equatorial SST gradient, and remote forcing from the eastern equatorial Pacific. *J. Geophys. Res.*, **107**, 10.1029/2000JD000307.

Czaja, A., P. van der Vaart, and J. Marshall, 2002: A diagnostic study of the role of remote forcing in tropical Atlantic variability. *J. Climate*, **15**, 3280–3290.

Dijkstra, H.A. and J.D. Neelin, 1995: Ocean-atmosphere interaction and the tropical climatology. Part II: Why the Pacific cold tongue is in the east. *J. Climate*, **8**, 1343–1359.

Enfield, D.B. and D.A. Mayer, 1997: Tropical Atlantic SST variability and its relation to El Nino-Southern Oscillation. *J. Geophys. Res.*, **102**, 929–945.

———, A.M. Mestas-Nunez, D.A. Mayer, and L. Cid-Serrano, 1999: How ubiquitous is the dipole relationship in tropical Atlantic sea surface temperatures? *J. Geophys. Res.*, **104**, 7841–7848.

Fedorov, A.V. and S.G.H. Philander, 2000: Is El Nino changing? *Science*, **288**, 1997–2002.

Gill, A.E., 1980: Some simple solutions for heat-induced tropical circulation. *Quart. J. Roy. Meteor. Soc.*, **106**, 447–462.

Hastenrath, S., 1991: *Climate dynamics of the tropics*. Kluwer Academic, Boston, USA, 488p.

Houghton, R.W. and Y.M. Tourre, 1992: Characteristics of low-frequency sea surface temperature fluctuations in the tropical Atlantic. *J. Climate*, **5**, 765–770.

Inatsu, M., H. Mukougawa, and S.-P. Xie, 2002: Stationary eddy response to surface boundary forcing: Idealized GCM experiments. *J. Atmos. Sci.*, **59**, 1898–1915.

Kimoto, M. and X. Shen, 1997: Climate variability studies using general circulation models. In *The Frontiers of Climate Research II*, A. Sumi Ed., 91–116, CCSR/Univ. of Tokyo.

Klein, S., B.J. Soden, and N.-C. Lau, 1999: Remote sea surface temperature variations during ENSO: Evidence for a tropical atmospheric bridge. *J. Climate*, **12**, 917–932.

Li, T., 1997: Air-sea interactions of relevance to the ITCZ: Analysis of coupled instabilities and experiments in the hybrid coupled GCM. *J. Atmos. Sci.*, **54**, 134–147.

Ma, C.-C., C.R. Mechoso, A.W. Robertson, and A. Arakawa, 1996: Peruvian stratus clouds and the tropical Pacific circulation—a coupled ocean-atmosphere GCM study. *J. Climate*, **9**, 1635–1645.

Matsuno, T., 1966: Quasi-geostrophic motions in the equatorial area. *J. Meteor. Soc. Japan*, **44**, 25–43.

Mechoso, C.R., A.W. Robertson, and Coauthors, 1995: The seasonal cycle over the tropical Pacific in general circulation models. *Mon. Wea. Rev.*, **123**, 2825–2838.

Mehta, V.M., 1998: Variability of the tropical ocean surface temperatures at decadal-multidecadal timescales. Part I: The Atlantic ocean. *J. Climate*, **11**, 2351–2375.

Miller, M.J., A.C.M. Beljaars, and T.N. Palmer, 1992: The sensitivity of the ECMWF model to the parameterization of evaporation from the tropical oceans. *J. Climate*, **5**, 418–434.

Mitchell, T.P. and J.M. Wallace, 1992: The annual cycle in equatorial convection and sea surface temperature. *J. Climate*, **5**, 1140–1156.

Neelin, J.D., D.S. Battisti, A.C. Hirst, F.-F. Jin, Y. Wakata, T. Yamagata, and S. Zebiak, 1998: ENSO theory. *J. Geophys. Res.*, **103**, 14261–14290.

Nobre, P. and J. Shukla, 1996: Variations of sea surface temperature, wind stress, and rainfall over the tropical Atlantic and South America. *J. Climate*, **9**, 2464–2479.

Numaguti, A., M. Takahashi, T. Nakajima, and A. Sumi, 1995: Description of CCSR/NIES atmospheric general circulation model. In *Climate System Dynamics and Modeling*, T. Matsuno Ed., CCSR/Univ. of Tokyo.

———, 1999: Origin and recycling processes of precipitating water over the Eurasian continent: Experiments using an atmospheric general circulation model. *J. Geophys. Res.*, **104**, 1957–1972.

Okumura, Y., S.-P. Xie, A. Numaguti, and Y. Tanimoto, 2001: Tropical Atlantic air-sea interaction and its influence on the NAO. *Geophys. Res. Lett.*, **28**, 1507–1510.

——— and ———, 2003: Atmospheric response to tropical Atlantic SST anomalies: Role of planetary boundary layer adjustment. *Proc. 12th Conf. on Interaction of the Sea and Atmos.*, P2.1, 1–7, Amer. Meteor. Soc., Long Beach.

Philander, S.G.H., D. Gu, D. Halpern, G. Lambert,

N.-C. Lau, T. Li, and R.C. Pacanowski, 1996: Why the ITCZ is mostly north of the equator. *J. Climate*, **9**, 2958–2972.

Rajagopalan, B., Y. Kushnir, and Y. Tourre, 1998: Observed decadal midlatitude and tropical Atlantic climate variability. *Geophys. Res. Lett.*, **25**, 3967–3970.

Seager, R., Y. Kushnir, M. Visbeck, N. Naik, J. Miller, G. Krahmann, and H. Cullen, 2000: Causes of Atlantic ocean climate variability between 1958 and 1998. *J. Climate*, **13**, 2845–2862.

Servain, J., 1991: Simple climate indices for the tropical Atlantic ocean and some Applications. *J. Geophys. Res.*, **96**, 15137–15146.

Sutton, R.T., S.P. Jewson, and D.P. Rowell, 2000: The elements of climate variability in the tropical Atlantic region. *J. Climate*, **13**, 3261–3284.

Sutton, R.T., W.A. Norton, and S.P. Jewson, 2001: The North Atlantic Oscillation—What role for the ocean? *Atmospheric Science Letters*, **10**.1006/2000.0018.

Tanimoto, Y. and S.-P. Xie, 1999: Ocean-atmospheric variability over the pan-Atlantic basin. *J. Meteor. Soc. Japan*, **77**, 31–46.

——— and ———, 2002: Inter-hemispheric decadal variations in SST, surface wind, heat flux and cloud cover over the Atlantic Ocean. *J. Meteor. Soc. Japan*, **80**, 1199–1219.

Wang, B. and S.-I. An, 2002: A mechanism for decadal changes of ENSO behavior: Roles of background wind changes. *Clim. Dyn.*, **18**, 475–486.

Wang, C., R.H. Weisberg, and J.I. Virmani, 1999: Western Pacific interannual variability associated with the El Nino Southern Oscillation. *J. Geophys. Res.*, **104**, 5131–5149.

Xie, S.-P. and S.G.H. Philander, 1994: A coupled ocean-atmosphere model of relevance to the ITCZ in the eastern Pacific. *Tellus*, **46A**, 340–350.

———, 1996: Westward propagation of latitudinal asymmetry in a coupled ocean-atmosphere model. *J. Atmos. Sci.*, **53**, 3236–3250.

———, 1997: Unstable transition of the tropical climate to an equatorially asymmetric state in a coupled ocean-atmosphere model. *Mon. Wea. Rev.*, **125**, 667–679.

———, 1998: Ocean-atmosphere interaction in the making of the Walker circulation and the equatorial cold tongue. *J. Climate*, **11**, 189–201.

———, 1999: A dynamic ocean-atmosphere model of the tropical Atlantic decadal variability. *J. Climate*, **12**, 64–70.

——— and Y. Tanimoto, 1998: A pan-Atlantic decadal climate oscillation. *Geophys. Res. Lett.*, **25**, 2185–2188.

———, Y. Tanimoto, H. Noguchi, and T. Matsuno, 1999: How and why climate variability differs between the tropical Pacific and Atlantic. *Geophys. Res. Lett.*, **26**, 1609–1612.

——— and K. Saito, 2001: Formation and variability of a northerly ITCZ in a hybrid coupled AGCM: Continental forcing and ocean-atmospheric feedback. *J. Climate*, **14**, 1262–1276.

Yukimoto, S., M. Endoh, Y. Kitamura, A. Kitoh, T. Motoi, and A. Noda, 2000: ENSO-like interdecadal variability in the Pacific ocean as simulated in a coupled genaral circulation model. *J. Geophys. Res.*, **105**, 13945–13963.

Zebiak, S.E. and M.A. Cane, 1987: A model El Nino-Southern Oscillation. *Mon. Wea. Rev.*, **115**, 2262–2278.